SORA vs. Euler angles: Computational Efficiency in the Context of Gyroscope Measurements

Sara Stančin*, Sašo Tomažič**
University of Ljubljana, Faculty of electrical engineering, Ljubljana, Slovenia
* sara.stancin@fe.uni-lj.si
** saso.tomazic@fe.uni-lj.si

Abstract— **We investigate the computational complexity of tracking 3D orientation (3DO) using gyroscope angular velocity measurements around its three sensitivity axes. These three rotations, obtained at every measurement step, are simultaneous and, due to rotation non-commutativity, interpreting them as sequential, i.e., Euler rotations, yields a systematic error in the estimated 3DO. As this error grows with the angle of rotation, an efficient approach for its reduction is to shorten the measurement interval, demanding a larger number of measurement and hence computational steps. We show that from the computational complexity point of view, for similar levels of result accuracy, the simultaneous interpretation of gyroscope measurements is superior to the sequential. Experimental results obtained using a dedicated microcontroller and relying on a specially developed, computationally optimized implementation, show that for the largest rotation angle considered, i.e., 3.67°, execution time for the simultaneous interpretation is 12 times shorter than for the sequential. Aiming to achieve computational efficiency and relevant comparison of both interpretations, rotation matrices were used when calculating 3DO after each measurement step and the rotation quaternions were used when combining multiple consecutive measurements in a single rotation composite.**

I. INTRODUCTION

A 3D gyroscope measures three angular velocities, each around a different sensitivity axis. The three sensitivity axes are mutually orthogonal; appropriately combining these three angular velocities enables angular orientation computation in the 3D reference frame.

With the ongoing developments in gyroscope manufacturing technology the use of these sensors in various fields is observably increasing: 3D gyroscopes are an integral component of inertial navigation units, they have been shown feasible for motion capture, classification, and analysis, and are essential elements of the assistive, rehabilitative and wearable health technology [1-15].

In our previous work [16-17], we have focused on the accuracy of the results obtained using 3D gyroscope measurements for angular orientation calculation. We demonstrated that, in general, significant improvement in the angular orientation accuracy can be achieved if the measured angular velocities are correctly interpreted as simultaneous and not as sequential rotations.

Due to different sources of motion sensor inaccuracies, accurate position estimation is a delicate task. Erroneous interpretation of the values measured with a 3D gyroscope only extends the deleterious effects on the estimated position of the sensor. Estimating the angular orientation by interpreting the three simultaneous rotations as sequential, i.e., Euler, may seem straightforward. However, the angles measured with a gyroscope are not, in general, equal to the angles of the elemental Euler rotations. In [17] we have shown that not only is interpreting simultaneous rotations as sequential theoretically erroneous, it introduces a significant systematic error in the angular orientation when the rotation angles become large.

For a rotation rate of 360°/s when sampled at 2.048 Hz the angular orientation error exceeds 6° after one minute of rotation. For the lowest sampling rate considered (4 Hz) for the same motion, the computed angular orientation is entirely unreliable as the error exceeds 73° after only one second of rotation. We have shown that significant accuracy improvements can be achieved in the real-case measurement scenario in which this systematic error only extends the deleterious effects of sensor inaccuracies in a noisy environment.

We have also shown that with appropriate 3D orientation computation implementation, significant reductions in time- and power-consumption can be achieved. With the described implementation we have achieved 14 times faster angular orientation calculation as oppose to an implementation with floating point arithmetic and library function calls (for estimating the square, inverse square, sine and cosine functions values). Both or these implementations were however shown to be suitable for real-time calculation for a single 3D sensor. However, in a wearable context multiple sensors can be used; reducing the duration of computation and improving computational efficiency can bring to prolonged energy autonomy of the computing devices.

In this article we further focus on the demands of the wearable device context. We investigate the effects of both interpretations of gyroscope measurements on 3DO computation execution time.

One of the challenges when using wearable devices is dictated by limited resources and the desired prolonged energy autonomy of the included devices. Any computation performed in the wearable context must oblige to low-power consumption demands. Further on, in

most application scenarios, results and feedback are needed in real-time.

By focusing on the aforementioned demands for the wearable device context, we investigate here the possibility of calculating angular orientation from 3D gyroscope measurements in real-time and in a low power consumption scenario.

It is our hypothesis that with appropriate implementation, significant reductions in time- and power-consumption can be achieved.

II. METHODOLOGY

To mutually compare the computational complexities for SORA and Euler angles interpretations at the same level of result accuracy, we designed the following experiment. We considered simulated 3D gyroscope measurements, affected by random measurement noise. We considered the sensor to be calibrated and that other sources of measurement inaccuracies, including output bias drift, inaccurate sensitivities and alignments of the sensor sensitivity axes are appropriately compensated for.

We considered the sensor to rotate with a particular level of angular velocity magnitude $\overline{\omega}$. We further considered the rotation axis to randomly oscillate around the value $[\ 1\ \ 1\ \ 1\ ]^T/\sqrt{3}$. Due to rotation noncommutativity, for a particular level of angular velocity magnitude, rotations around the axis $[\ 1\ \ 1\ \ 1\ ]^T/\sqrt{3}$ lead, in general, to the largest error in the resulting 3DO calculated by relying on Euler angles. Such a condition is not uncommon and it is our aim here to investigate the associated computational efficiency.

Adding the measurement noise for each step $1 \le n \le N$, the simulated angular velocity measurements for each axis respectively, i.e., $\omega_{s,x}[n]$, $\omega_{s,y}[n]$, and $\omega_{s,z}[n]$, were obtained according to the following expressions:

$$\begin{aligned}\omega_{s,x}[n] &= \overline{\omega}/\sqrt{3}(1+\sigma_x[n])+\eta_{s,x}[n],\\ \omega_{s,y}[n] &= \overline{\omega}/\sqrt{3}(1+\sigma_z[n])+\eta_{s,y}[n],\\ \omega_{s,z}[n] &= \overline{\omega}/\sqrt{3}(1+\sigma_y[n])+\eta_{s,z}[n],\end{aligned} \tag{1}$$

where $\sigma_x[n]$, $\sigma_y[n]$, and $\sigma_z[n]$ denote random oscillations in the sensor's angular velocity and the rotation axis, generated to have normal distribution with zero mean and standard deviation equal to 0.1. $\eta_{s,x}[n]$, $\eta_{s,y}[n]$, and $\eta_{s,z}[n]$ denote measurement noise for each sensitivity axis of the sensor, generated to have normal distribution with zero mean and standard deviation equal to $1^\circ\ s^{-1}$.

To compare 3DO accuracy and computational complexities for different levels of the measured angular velocity, we considered eleven different trials of the experiment, for each increasing the level of the sensor's rotation $\overline{\omega}$ from $5^\circ\ s^{-1}$ to $55^\circ\ s^{-1}$ with an incremental step of $5^\circ\ s^{-1}$.

Using the generated values (1), we calculated the 3DO for each considered angular velocity level $\overline{\omega}$ for both A) step-wise and B) final 3DO, each for both gyroscope measurement interpretations for all eleven trials after τ = 10 s of rotation. Setting the sampling frequency to f_s = 15 Hz gave us $N = f_s\,\tau = 150$ consecutive measurements. For the sampling frequency f_s = 15 Hz, increasing angular velocity in (1) from $5^\circ\ s^{-1}$ to $55^\circ\ s^{-1}$ by a step of $5^\circ\ s^{-1}$ brings to an increase of the rotation angle from 0.33° to 3.63° by an incremental step of 0.33°.

Relying on the optimal computation methods for A) step-wise 3DO calculation, the results were calculated using rotation matrices. Relying on the optimal computation methods for B) step-wise 3DO calculation, the results were calculated using rotation quaternions.

We designed and developed a c/c++ angular orientation computation program. We executed the experimental angular orientation calculation using an Arduino Zero board [18]. The board itself includes a 32-bit ARM Cortex® M0+ microcontroller [19] developed by Atmel. The microcontroller has a clock speed of 48 MHz, 32 KB of SRAM and 256 KB of flash memory. The used testing Arduino board does not include a floating-point computational unit and supports low power consumption. This characteristic makes the microcontroller itself appropriate for the wearable device context where energy autonomy is important and to which we wanted to adapt our experiment and relate our findings.

We used integer arithmetic exclusively. By using integer arithmetic exclusively, we avoided general floating point to integer conversions and so achieved greater computational efficiency and, consequently, more reliable and meaningful comparison results.

Further on, we implemented the square root and inverse square root functions estimations as a combination of lookup table value retrieval and linear interpolation. Both lookup-tables were designed to give the highest accuracy and still fit into the available SRAM of the microcontroller.

We considered limited measurement accuracy up to two decimal places as well as a limited range of the measured angular velocity. The range of the input values and both lookup tables was chosen to fit into the available 32 KB of working memory.

Finally, we implemented the sine and cosine function evaluations using the small angle approximation.

III. RESULTS

We evaluated the results accuracy with respect to the 3DO values obtained by considering noiseless measurements, i.e. by setting:

$$\eta_{s,x}[n]=0,\ \eta_{s,y}[n]=0,\ \eta_{s,z}[n]=0 \tag{2}$$

in (1). Double float precision was used for this calculation. We estimated the accuracy of the final results for both, SORA and Euler angles, as the number of accurate decimal places.

The systematic error introduced with the Euler rotations interpretation is expected to grow with the angle of each consecutive rotation measurement φ. For a specific angular velocity value, the shorter the measurement interval T_s, the smaller the error. Hence, for each experiment trial we increased the sampling frequency for Euler angles as much as was needed to obtain results at the same level of accuracy as were obtained for SORA.

By finally measuring the execution times we were able to obtain reliable computational complexity comparison of both interpretations at a similar level of accuracy of the final 3DO results. As a final measure of computational efficiency for A) and B), we used the ratio between the execution times for SORA and Euler angles for each of the eleven trials:

$$r = \Delta t_{zyx} / \Delta t_{\text{sim}}, \quad (3)$$

where Δt_{zyx} and Δt_{sim} denote the execution times for the Euler angles and SORA.

For both 3DO calculation scenarios, A) step-wise 3DO and B) only final, for the sampling frequency f_s = 15 Hz the results for SORA were accurate up to the second decimal place, for all rotation angles considered. For Euler angles, the results were accurate up to the second decimal place only for the three smallest angular velocity values considered, i.e. 5° s^{-1}, 10° s^{-1}, and 15° s^{-1}. For these, the execution times for Euler angles for A) were shorter than those for the SORA interpretation ($r^{(A)}$ = 0.90), as was expected due to already established fewer number of computational operations per equal number of measurement steps. For B) the execution times for Euler angles slightly exceed the execution times for the SORA interpretation ($r^{(B)}$ = 1.06), reflecting the use of rotation quaternions instead of rotation matrices and being in full accordance with the theoretical results.

However, as the angular velocity levels grew from the third to the eleventh trial of the experiment, the accuracy of the results for the Euler angles deteriorate significantly and the sampling frequency had to be increased ever more in order to obtain results at the same level of accuracy as was obtained for SORA. While the execution times for SORA remained equal for all eleven trials, this increase in the sampling frequency led to longer execution times for the Euler angles. The obtained execution times ratios are presented in Figure 1. For the largest angular velocity value considered, i.e. 55° s^{-1}, the sampling frequency had to be increased to 210 Hz for A) and to 170 Hz for B), leading to around 12 times ($r^{(A)}$=12.39, $r^{(B)}$ = 11.85) longer execution time for the Euler rotations than for SORA.

In the special case when the 3D gyroscope is rotating around one of its intrinsic coordinate axis, both SORA and Euler angles interpretations are equivalent. Comparing for each calculation method, the 3DO calculation equations are in this special case identical for both, SORA and Euler angles. For SORA and Euler angles we so obtain equal 3DO results with the same computational efficiency.

However, in all other cases, Euler angles introduce an error in the calculated 3DO. To obtain comparably accurate results, more computational steps are required. Afore presented results show that computational efficiency of using SORA as oppose to using Euler angles grows with the measured angular velocity values, as for comparable levels of result accuracy, lower sampling frequencies are required.

As a final note - by eliminating the random angular velocity components $\sigma_x[n]$, $\sigma_y[n]$, and $\sigma_z[n]$ in (1), the rotation axis becomes constant (up to the effect or random measurement noise) for all N measurement steps. Under such a condition, using SORA, we can combine all measurements and calculate 3DO in a single step. On the contrary, doing the same for Euler angles would result in even larger error in the computed 3DO, due to a larger rotation angle considered. We can hence conclude that, depending on for how long the sensor rotates around a constant axis, execution time can be drastically reduced by interpreting the measured gyroscope values using SORA.

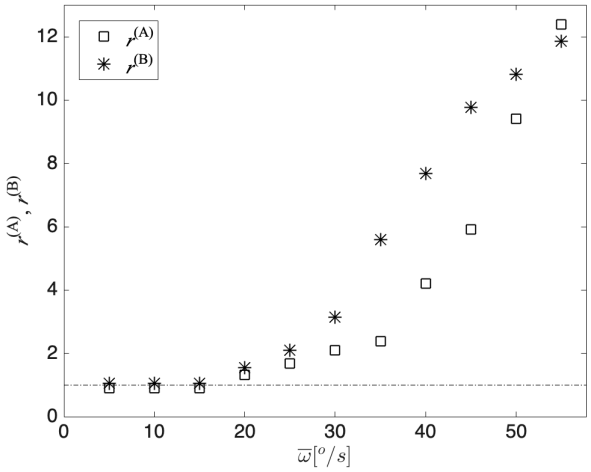

Figure 1. Execution time efficiency r of using SORA vs. Euler angles for calculating 3DO using gyroscope measurements at a comparable level of result accuracy. $r^{(A)}$ and $r^{(B)}$ refer to step-wise and only final 3DO calculation, respectively. Values close to 1 for the three smallest angular velociy values (5° s^{-1}, 10° s^{-1}, and 15° s^{-1}) imply comparable execution times. For ever larger angular velocity levels, Euler angles demand ever higher sampling frequencies, leading to ever longer execution times and higher values of both $r^{(A)}$ and $r^{(B)}$. For the largest angular velocity value, i.e., 55° s^{-1}, the execution time for the sequential rotation interpretation was $r^{(A)}$=12.39 and $r^{(B)}$=11.85 times longer.

IV. CONCLUSIONS

To investigate the differences in the computational complexities of different angular orientation calculation methods, we have implemented angular orientation calculation on a dedicated low-power microcontroller. Considering the absolute time-consumption, we concluded that all calculation methods are well suited for real-time angular orientation calculation with the specific 32-bit ARM Cortex® M0+ microcontroller. However, by applying the more appropriate angular orientation computation approach, significant reduction of execution time can be achieved.

To evaluate the advantage of the simultaneous vs. the sequential rotation interpretation with respect to computational efficiency, we investigated the sampling frequency needed for both approaches that bring to similar magnitudes of errors in the computed angular orientation. The results have shown that, for the simultaneous rotation interpretation the same level of result accuracy can be achieved with significantly lower sampling frequencies, leading to a significant reduction in computational complexity and execution time. Following this reasoning, for the specific 3D gyroscope context, the simultaneous elemental rotations interpretation should be preferred over the sequential.

To finally conclude, by adopting the practices presented in this manuscript, prolonged energy autonomy of the computing device can be achieved, enhancing its usability

in an every-day measurement scenario and an ubiquitous context.

REFERENCES

[1] J. Lee, H. Joo, J. Lee, Y. Chee, "Automatic Classification of Squat Posture Using Inertial Sensors: Deep Learning Approach", *Sensors,* 2020, *20*, 361.

[2] A. Martínez, R. Jahnel, M. Buchecker, C. Snyder, R. Brunauer, T. Stöggl, "Development of an Automatic Alpine Skiing Turn Detection Algorithm Based on a Simple Sensor Setup", *Sensors*, 2019, *19*, 902.

[3] L. Benages Pardo, D. Buldain Perez, C. Orrite Uruñuela, "Detection of Tennis Activities with Wearable Sensors", *Sensors*, 2019, *19*, 5004.

[4] S. Stančin, S. Tomažič, "Early improper motion detection in golf swings using wearable motion sensors: The first approach", *Sensors*, 2013, *13*, 7505–7521.

[5] A. Umek, A. Kos, "Validation of smartphone gyroscopes for mobile biofeedback applications", *Pers. Ubiquit. Comput.*, 2016, *20*, 657–666.

[6] P.C. Formento, R. Acevedo, S. Ghoussayni, D. Ewins, "Gait Event Detection during Stair Walking Using a Rate Gyroscope", *Sensors*, 2014, *14*, 5470–5485.

[7] T. Seel, J. Raisch, T. Schauer, "IMU-Based joint angle measurement for gait analysis", *Sensors*, 2014, *14*, 6891–6969.

[8] E. Allseits, K.J. Kim, C. Bennett, R. Gailey, I. Gaunaurd, V. Agrawal, "A Novel Method for Estimating Knee Angle Using Two Leg-Mounted Gyroscopes for Continuous Monitoring with Mobile Health Devices", *Sensors*, 2018, *18*, 2759.

[9] A. Umek, A. Kos, A., S. Tomažič, "Validation of smartphone gyroscopes for angular tracking in biofeedback applications", In Proceedings of the 2015 International Conference on Identification, Information, and Knowledge in the Internet of Things, Beijing, China, 22–23 October 2015.

[10] A. M. Sabatini, "Estimating three-dimensional orientation of human body parts by inertial/magnetic sensing", *Sensors*, 2011, *11*, 1489–1525.

[11] D. T. P. Fong, Y. Y. Chan, "The use of wearable inertial motion sensors in human lower limb biomechanics studies: A systematic review", *Sensors*, 2010, *10*, 11556–11565.

[12] K. A. Pratt, S. M. Sigward, "Inertial Sensor Angular Velocities Reflect Dynamic Knee Loading during Single Limb Loading in Individuals Following Anterior Cruciate Ligament Reconstruction", *Sensors*, 2018, *18*, 3460.

[13] O. Herrera-Alcántara, A. Y. Barrera-Animas, M. González-Mendoza, F. Castro-Espinoza, "Monitoring Student Activities with Smartwatches: On the Academic Performance Enhancement", *Sensors*, 2019, *19*, 1605.

[14] J. A. Gallego, E. Rocon, J. O. Roa, J. C. Moreno, J. L. Pons, "Real-Time Estimation of Pathological Tremor Parameters from Gyroscope Data", *Sensors*, 2010, *10*, 2129–2149.

[15] A. Ali, N. El-Sheimy, "Low-Cost MEMS-Based Pedestrian Navigation Technique for GPS-Denied Areas", *J. Sens.*, 2013, *2013*, doi:10.1155/2013/197090.

[16] S. Stančin, S. Tomažič, "Angle estimation of simultaneous orthogonal rotations from 3D gyroscope measurements", *Sensors*, 2011, *11*, 8536–8549.

[17] S. Stančin, S. Tomažič, "On the interpretation of 3D gyroscope measurements", *J. Sens.*, 2018, *2018*, doi:10.1155/2018/9684326.

[18] Arduino Zero Technical Specification. Available online: https://store.arduino.cc/genuino-zero (accessed on 28 October 2019.)

[19] SMART ARM-based Microcontroller Datasheet. Available online: https://cdn.sparkfun.com/datasheets/Dev/Arduino/Boards/Atmel-42181-SAM-D21_Datasheet.pdf (accessed on 28 October 2019.)